Figure 4 presents comparison of the effects of specific heat ratio for a cone angle of 20°. Both approximations are close for shock angle and surface Mach number, but the approximation of Ref. 1 shows appreciable error in surface pressure coefficient, even for $M_\infty = 20$.

Approximations for shock wave angle and surface pressure coefficient, which can be used for all Mach numbers and for cone angles from zero to the detachment value, have been determined for the case of a cone at zero angle of attack in supersonic flow. Comparisons with exact results indicate that the precision is adequate for engineering purposes.

References

[1] Hammitt, A. G. and Murthy, K. R. A., "Approximate solutions for supersonic flow over wedges and cones," J. Aerospace Sci. 27, 71–72 (1960).

[2] "Equations, tables, and charts for compressible flow," Ames Res. Lab., NACA Rept. 1135, pp. 48–53 (1953).

Travel Summation and Time Summation Methods of Free-Oscillation Data Analysis

KAZIMIERZ J. ORLIK-RÜCKEMANN*
National Aeronautical Establishment, Ottawa, Ontario, Canada

THERE are many instances, e.g., when performing wind tunnel studies of the dynamic behavior of re-entry configurations, where experiments involving very large amplitudes of oscillation are of interest. In such cases, it may be difficult to obtain data in the convenient form of an analog output of the displacement-time history, and hence the instantaneous methods of data reduction such as the dampometer method[1] or the integration method[2] cannot be used. The two methods described herein do not require analog outputs yet still permit instantaneous reduction of free-oscillation data. They are both based on the concept of viscous damping and thus present results in terms of the equivalent viscous damping.

Travel Summation Method

It will be shown here, that if the sum of all the travel segments between two preset levels of displacement of a free decaying oscillation is known, the logarithmic decrement corresponding to the equivalent viscous damping can be obtained from a simple analytical expression.

In order to visualize more easily the problem, one can consider the simplest form of many possible experimental arrangements, namely an oscillating light source seen through a stationary window, as schematically presented in Fig. 1. The length of the window and its position are such that the light source can be seen only during a portion of each cycle, namely when its deflection from equilibrium is between x_0 and x_m. When the amplitude of oscillation decreases below x_m the light source is cut off. The total visible travel of the light source in relation to the window is recorded. This can be done, e.g., by replacing the window with a large number of fine transversal slots and recording the total number of resulting light pulses on a photomultiplier tube. The procedure, of course, can be applied to both translational and angular oscillatory motions; it can be reversed by keeping

Received April 22, 1963.

* Head, Unsteady Aerodynamics Laboratory. Associate Fellow Member AIAA.

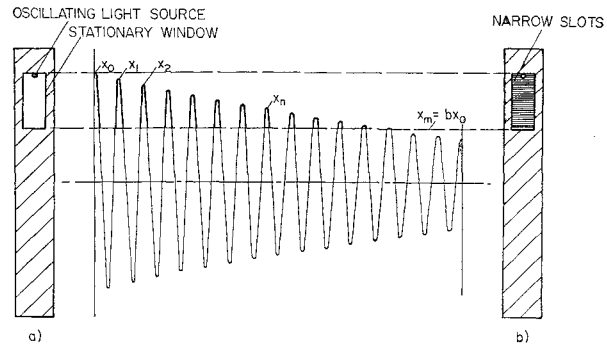

Fig. 1 Free oscillation data analysis using a) time summation method [Eqs. (9, 10, and 13)] and b) travel summation method [Eqs. (3, 4, and 7)]

the light source stationary and oscillating the slotted window; it can be modified by keeping both the light source and the slotted window stationary and oscillating suitably located mirrors. Numerous experimental arrangements are possible, but their detail aspects will not be elaborated here.

Thus, if the upper limit of the amplitude range under consideration is x_0 and the lower limit is x_m, one has, for a free-oscillation motion with viscous damping,

$$x_m = e^{-m\delta}x_0 = c^m x_0 = bx_0 \tag{1}$$

where m denotes the number of cycles between x_0 and x_m and $c = e^{-\delta}$ is a convenient constant related to the amount of viscous damping; δ denotes the logarithmic decrement. The amplitude of the nth peak between x_0 and x_m similarly can be written as

$$x_n = c^n x_0 \tag{2}$$

Assuming that the oscillation starts at x_0, the sum S of all the travel segments contained between x_0 and x_m is

$$S = 2\sum_{n=0}^{m}(x_n - x_m) - (x_0 - x_m) \tag{3}$$

Inserting Eqs. (1) and (2) and expressing the total travel S in terms of the initial amplitude x_0, one obtains

$$s = \frac{S}{x_0} = 2\sum_{n=0}^{m} c^n - (2m+1)b - 1 \tag{4}$$

Replacing the geometric progression on the right-hand side by its sum and solving for c, one gets

$$c = \frac{s + (2m+1)b - 1}{s + (2m+1)b - 2b + 1} = \frac{1 - [(1-b)/(s+2mb)]}{1 + [(1-b)/(s+2mb)]} \tag{5}$$

The logarithmic decrement now can be obtained from

$$\delta = \ln\frac{1}{c} = 2\left[\left(\frac{1-b}{s+2mb}\right) + \frac{1}{3}\left(\frac{1-b}{s+2mb}\right)^3 + \dots\right] \tag{6}$$

where for most applications only the first term of the logarithmic expansion need be retained. The resulting error is less than 0.1% for $\delta < 0.1$ and less than 0.8% for $\delta < 0.3$.

Using the relation between m, b, and δ given by Eq. (1), m can be eliminated, which leads to the final expression for the logarithmic decrement

$$\delta = (2/s)(1 - b + b\ln b) \tag{7}$$

For a given experimental arrangement b is fixed (with convenient values around 0.5), and thus the logarithmic decrement is simply obtained by dividing a constant by the dimensionless sum s of the travel segments. It should be noted that, since a change in b causes a change in the travel segment

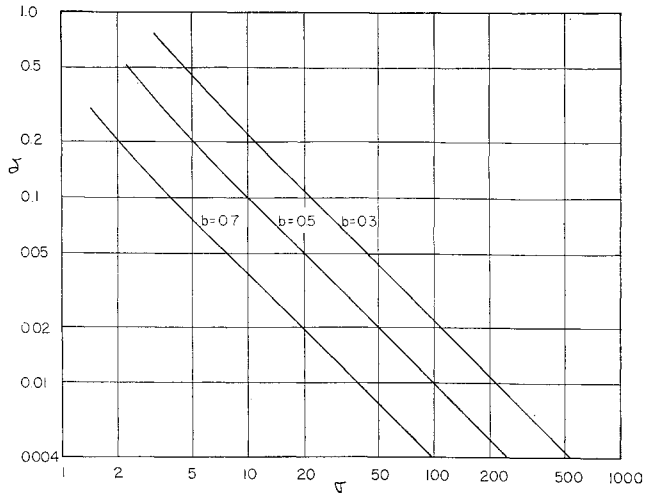

Fig. 2 Time summation method; graphical solution of Eq. (10)

of each cycle and not only in the final cycle, the result of travel summation varies smoothly with b and does not depend critically on m being an integer. It can be shown that the maximum pertinent error, which only will occur if the cut-off takes place approximately half-way between two peaks, can be expressed as

$$\Delta\delta/\delta = -(b/s)[(2m + 1)(1 - c^{1/2}) + \ln b] \qquad (8)$$

which, for a typical example of $\delta = 0.05$ and $b = 0.535$, gives a value of 0.25%. If necessary, this error can be reduced by proper selection of b. Since the error due to a final resolution of the slotted window can be made negligible with suitable experimental arrangements, the total error, including the approximation involved in retaining only one term in Eq. (6), can be kept under 1% in most practical cases.

Time Summation Method

For some applications, where it may be difficult to measure accurately the sum of all the travel segments between two levels of displacement as just discussed, it may be better to measure instead the sum of all the time intervals for the consecutive cycles of oscillation during which the motion is contained between the two limiting levels of displacements. Introducing again the example of the relative motion between a light source and a window (Fig. 1), such a measurement requires a photomultiplier tube activating and deactivating an electronic timer until the amplitude decreases below the cut-off level.

To obtain a simple expression for the time it takes to travel from the cut-off level x_m to the peak x_n of each successive cycle and back, consider each cycle as undamped motion, with damping affecting only the amplitude of the successive peaks. As compared to undamped motion, the time to move from x_m to x_n is somewhat shorter and the time to move from x_n back to x_m is somewhat longer when the motion is damped; hence the effect of this approximation on the sum of these two time intervals, which is the main concern here, is very small. Thus one can write

$$x_m = x_n \cos\omega t_n = c^n x_0 \cos\omega t_n \qquad (9)$$

where $2t_n$ denotes the time to travel from x_m to x_n and back to x_m.

Assuming again that the oscillation starts at x_0, inserting Eqs. (1) and (2), and introducing a dimensionless sum of all the successive time intervals $2t_n$, one obtains

$$\sigma = \omega\left[\sum_{n=0}^{m} 2t_n - t_0\right] = \sum_{n=0}^{m} 2\cos^{-1}(bc^{-n}) - \cos^{-1}b \qquad (10)$$

where the first term on the right-hand side can be expanded in the series:

$$\sum_{n=0}^{m} 2\cos^{-1}(bc^{-n}) = \pi(m + 1) - 2\sum_{n=0}^{m}\left(\frac{b}{c^n}\right) - \frac{1}{3}\sum_{n=0}^{m}\left(\frac{b}{c^{3n}}\right) - \ldots \qquad (11)$$

By following an analysis similar to that leading to Eq. (7), one finally obtains

$$\delta = \frac{-\pi \ln b - 2(1 - b)}{\sigma + 1 - (\pi/2)} \qquad (12)$$

The series expansion of Eq. (11) converges, however, rather slowly, which renders Eq. (12) too inaccurate for practical applications. For accurate results Eq. (10) must be solved graphically. Such a solution is presented in Fig. 2 for three representative values of b; once σ is known, the logarithmic decrement δ can be obtained immediately from this diagram.

The curves in Fig. 2 can be represented analytically by the following empirical modification of Eq. (12):

$$\delta = 2.63\left(\frac{1.8 - b}{4.6 - b}\right)\left(\frac{-\pi \ln b - 2(1 - b)}{\sigma - 0.2}\right) = \frac{f(b)}{\sigma - 0.2} \qquad (13)$$

where $f(b)$ is usually constant for a given experimental arrangement. Equation (13), which is far more convenient to use than the diagram in Fig. 2, can be applied to any value of b within the range indicated and gives an accuracy, as compared to an exact solution of Eq. (10), to better than 1% for $b = 0.3$ and $\delta \leqslant 0.5$ and to better than 3.5% for $0.3 \leqslant b \leqslant 0.7$ and $\delta \leqslant 0.3$.

In order to convert the actual time measured into the dimensionless time σ, the value of the oscillation frequency ω must be known. This quantity is easily obtainable from the experiments and in most cases also is required independently

Concluding Remarks

Because of the approximation preceding Eq. (9), which specially affects the first time interval t_0, the time summation method is inherently less accurate than the travel summation method and should not be used when drastically small values of m can be expected (i.e., when both b and δ are relatively large). For low values of δ, however, the time summation method may be preferable, since it usually permits simpler experimental arrangements.

As mentioned in the first paragraph of this note, the two new methods of free-oscillation data analysis described here represent a significant advance (as compared to all other methods, which use analysis of full cycles for data reduction) in obtaining instantaneous results of satisfactory accuracy in cases when an analog output of the displacement-time history is not available, which is often the case in experiments involving large amplitudes of oscillation. For small amplitudes the use of methods such as the dampometer method[1] is clearly more advantageous, since an analog output as a rule can be arranged easily and since the accuracy of the summation methods described here decreases markedly with decreasing amplitude range. Finally in the rare cases when amplitudes are large yet allowing an analog treatment, the choice depends largely on availability of equipment, both approaches giving instantaneous results of satisfactory accuracy.

References

[1] Olsson, C. O. and Orlik-Rückemann, K. J., "An electronic apparatus for automatic recording of the logarithmic decrement

and frequency of oscillations in the audio and subaudio frequency range," Aeronaut. Res. Inst. Sweden Rept. 52 (1954).

[2] Bratt, J. B., "Wind tunnel techniques for the measurement of oscillatory derivatives," Aeronaut. Res. Council England Paper 22, 146, pp. 13–14 (1960).

Thermal Stresses in Nonhomogeneous Thin Shells

B. Walter Rosen*
General Electric Company, King of Prussia, Pa.

Thermal stresses in nonhomogeneous, complete, thin shells of arbitrary shape and constant thickness are evaluated for the case where the temperature and the elastic constants are a function of only the local normal coordinate. The analysis shows that the thermal stresses in the local tangent plane are independent of the shape of the middle surface of the shell.

Introduction

THE design of high-temperature thermal protection systems for re-entry vehicles, rocket nozzles, and hypervelocity aircraft requires consideration of multilayered shells with large temperature variations through the shell thickness. The problem of thermal stresses in such structures has received considerable attention in recent years. The solutions for the most arbitrary geometry and temperature distributions are cumbersome and require considerable use of high-speed computing equipment. Such solutions are of limited value for the parametric studies necessary to design minimum weight vehicles, since they must be used in conjunction with equally complex aerothermodynamic analyses. The aim of this paper is to present the simple result of an analysis that treats a major aspect of these thermal stress problems in a fashion that makes it readily usable for the multiple analyses associated with system optimization.

Analysis

The problem to be treated is an arbitrary shape, closed, thin shell of constant thickness subjected to an arbitrary temperature distribution that varies through the thickness only. Mechanical properties of the shell may vary with respect to the local normal coordinate and also with respect to temperature. The material is treated as isotropic and elastic. The surface coordinate curves are selected to coincide with the lines of principal curvature of the surface. The local normal is taken as the direction of the third coordinate of this orthogonal coordinate system.

The radial stresses are neglected in the tangential stress-strain relations, which may be written as

$$\begin{aligned}\sigma_{11} &= [E/(1-\nu^2)][\epsilon_{11} + \nu\epsilon_{22} - (1+\nu)\epsilon_T]\\ \sigma_{22} &= [E/(1-\nu^2)][\epsilon_{22} + \nu\epsilon_{11} - (1+\nu)\epsilon_T]\\ \sigma_{12} &= [E/2(1+\nu)]\epsilon_{12}\end{aligned} \tag{1}$$

where E is Young's modulus, ν is Poisson's ratio; 1 and 2 are the principal directions, and ϵ_T is the free thermal expansion associated with the prescribed temperature changes.

Received May 6, 1963.

* Consulting Engineer, Space Sciences Laboratory. Member AIAA.

The equilibrium equations for an arbitrary thin shell are given by Novozhilov[1] as

$$\frac{\partial(A_2T_1)}{\partial\alpha_1} + \frac{\partial(A_1S)}{\partial\alpha_2} + S\frac{\partial A_1}{\partial\alpha_2} - T_2\frac{\partial A_2}{\partial\alpha_1} + \frac{1}{R_1}\left[\frac{\partial(A_2M_1)}{\partial\alpha_1} - M_2\frac{\partial A_2}{\partial\alpha_1} + 2\frac{\partial(A_1H)}{\partial\alpha_2} + 2H\frac{R_1}{R_2}\frac{\partial A_1}{\partial\alpha_2}\right] = -A_1A_2q_1$$

$$\frac{\partial(A_2S)}{\partial\alpha_1} + \frac{\partial(A_1T_2)}{\partial\alpha_2} + S\frac{\partial A_2}{\partial\alpha_1} - T_1\frac{\partial A_1}{\partial\alpha_2} + \frac{1}{R_2}\left[\frac{\partial(A_1M_2)}{\partial\alpha_2} - M_1\frac{\partial A_1}{\partial\alpha_2} + 2\frac{\partial(A_2H)}{\partial\alpha_1} + 2H\frac{R_2}{R_1}\frac{\partial A_2}{\partial\alpha_1}\right] = -A_1A_2q$$

$$\frac{T_1}{R_1} + \frac{T_2}{R_2} - \frac{1}{A_1A_2}\left\{\frac{\partial}{\partial\alpha_1}\frac{1}{A_1}\left[\frac{\partial(A_2M_1)}{\partial\alpha_1} + \frac{\partial(A_1H)}{\partial\alpha_2} + H\frac{\partial A_1}{\partial\alpha_2} - M_2\frac{\partial A_2}{\partial\alpha_1}\right] + \frac{\partial}{\partial\alpha_2}\frac{1}{A_2}\left[\frac{\partial(A_2H)}{\partial\alpha_1} + \frac{\partial(A_1M_2)}{\partial\alpha_2} + H\frac{\partial A_2}{\partial\alpha_1} - M_1\frac{\partial A_1}{\partial\alpha_2}\right]\right\} = q_n \tag{2}$$

where α_1 and α_2 are the surface coordinates, R_1 and R_2 are the principal radii of curvature, q_1, q_2, and q_n are the components of the applied pressure, A_1 and A_2 are Lamés parameters, defined by the metric form

$$(ds)^2 = (A_1d\alpha_1)^2 + (A_2d\alpha_2)^2$$

and T_1, T_2, T_{12}, and T_{21} are stress resultants, and M_1, M_2, M_{12}, and M_{21} are moment resultants defined by (for shell thickness h)

$$\begin{aligned}T_1 &= \int_{-h/2}^{h/2}\sigma_{11}dz & T_2 &= \int_{-h/2}^{h/2}\sigma_{22}dz\\ T_{12} &= \int_{-h/2}^{h/2}\sigma_{12}\left(1+\frac{z}{R_2}\right)dz & T_{21} &= \int_{-h/2}^{h/2}\sigma_{21}\times\left(1+\frac{z}{R_1}\right)dz\\ M_1 &= \int_{-h/2}^{h/2}\sigma_{11}zdz & M_2 &= \int_{-h/2}^{h/2}\sigma_{22}zdz\\ M_{12} &= \int_{-h/2}^{h/2}\sigma_{12}\left(1+\frac{z}{R_2}\right)zdz & M_{21} &= \int_{-h/2}^{h/2}\sigma_{21}\times\left(1+\frac{z}{R_1}\right)zdz\end{aligned} \tag{3}$$

$$H = \tfrac{1}{2}(M_{12} + M_{21})$$

$$S = T_{12} - (M_{21}/R_2) = T_{21} - (M_{12}/R_1)$$

Note that, although $z/R \ll 1$, the simplification that results from neglecting these terms in the shear force and twisting moment resultants introduces certain contradictions into the theory.[1] For this reason, such terms will be retained here, and the resultants are as defined in Eqs. (3).

It can be seen that, for no external load ($q_1 = q_2 = q_n = 0$), compatible displacements which yield equal, constant moment resultants in the two principal directions, and vanishing stress and twisting moment resultants, will satisfy the equilibrium equations (2) and thus be a solution to the problem. (Since a closed shell is considered, there are no further boundary conditions.) Such a solution is given by the uniform strain solution:

$$\epsilon_{11} = \epsilon_{22} = \frac{\int_{-h/2}^{h/2}\frac{E\epsilon_T}{1-\nu}dz}{\int_{-h/2}^{h/2}\frac{E}{1-\nu}dz} \tag{4}$$

$$\epsilon_{12} = 0$$